Ocean Engng, Vol. 19, No 2, pp. 139–159, 1992.
Printed in Great Britain.

0029–8018/92 $5.00 + .00
Pergamon Press plc

LAUNCH AND IMPACT OF FREE-FALL LIFEBOATS. PART II. IMPLEMENTATION AND APPLICATIONS

W. J. C. BOEF*

Shell Research B.V., Koninklijke/Shell Exploratie en Produktie Laboratorium, Rijswijk, The Netherlands

Abstract—There is a great interest in a practical method of predicting the behaviour of a free-fall lifeboat, when dropped from an offshore platform or from a ship, in order to assess the risk of injury to the occupants. In particular, for those environmental conditions in which full-scale experiments are very difficult, one can benefit from numerical prediction. The hydrodynamic impact of the boat at water entry is a complex problem and makes the establishment of an analytical prediction method a challenging task.

This paper is the second of two articles outlining a practical method for simulating the water entry of a free-fall lifeboat. The first article (Part I: impact theory) [BOEF, W. J. C. (1992), *Ocean Engng* **19**, 119–138] reviewed the relevant literature on hydrodynamic impact and outlined the theoretical model for the water entry of a lifeboat. This paper discusses the implementation of the lifeboat launch model and a method for evaluating the effects of impacts on the occupants. The results of a comparison with full-scale tests and of a case study are also included.

NOMENCLATURE

A_{da}, A_{dn}	cross-sectional areas for air drag, along and normal to the boat axis, respectively
a_x, a_z	acceleration at seat foundation along and normal to boat axis
$BH1$	height of wedge-shaped part of lifeboat's cross-section
$BH2$	height of rectangular part of lifeboat's cross-section
B_{XX}	distance along boat axis from cog to most forwards point of contact between boat and launch skid
B_{x1}	distance along boat axis from cog to start of line of contact
B_{x2}	distance along boat axis from cog to end of line of contact
B_z	height of boat's sliding beam above cog
C_{da}, C_{dn}	air drag coefficient along and normal to the boat axis
$CDRR$	combined dynamic response ratio; ratio between actual and allowable displacements of human body model
cog	centre of gravity of the lifeboat
F_{buoy}	buoyancy and wave inertia force on lifeboat
F_{drag}	hydrodynamic drag force along the axis of the boat
F_{mom}	total force on boat due to momentum transfer normal to boat axis
F_n	total normal reaction force exerted on the boat by the launch skid
F_{n1}	normal reaction force exerted on the boat by the launch skid at B_{xx}
F_{n2}	normal reaction force exerted on the boat by the launch skid at B_{x2}
F_{wx}	horizontal force on boat due to air (and wind) drag
F_{wz}	vertical force on boat due to air (and wind) drag
$FM_{...}$	moment on boat due to force $F_{...}$
g	acceleration due to gravity
H	drop height of boat (from bow to sea level)
I	moment of inertia of the lifeboat in plane of symmetry
L	length of boat model
M	total mass of the lifeboat with occupants
M_w	moment on boat due to air (and wind) drag
m_{ij}	ij-component of the added mass matrix of the lifeboat

*Presently with: Norsk Hydro a.s, Drammensveien 264, Vækerø, Oslo, P.O. Box 200, N-1321 Stabekk, Norway.

SL	length of launch skid from low end to cog of the boat
S_{fr}	friction factor between boat and skid
S_x,S_y,S_z	allowable relative displacement between body and set in x-, y- and z-directions, respectively
s	coordinate along boat axis (s = 0: stern of boat model)
s_{cog}	distance from stern to cog
s_s	distance from stern to seat
t	time
v_{ax},v_{nor}	velocity along and normal to boat axis (at cog)
v_x,v_z	horizontal and vertical velocity of lifeboat
v_{xx}	time derivative of δ_{xx}
$x,y,z,$	global coordinates
α	angle of launch skid with the vertical
$\delta_x,\delta_y,\delta_z$	relative displacement between body and seat in x-, y- and z-directions, respectively
δ_{xx}	δ_x in response to a_x
δ_{xz}	δ_x in response to a_z
δ_{zx}	δ_z in response to a_x
δ_{zz}	δ_z in response to a_z
$\delta_{*\phi}$	actual relative displacement between body and seat in *-direction (* = x,y,z) for a seat angle ϕ with the vertical
ρ_w	specific density of air
ϕ	angle between boat axis and vertical (ϕ = 0: "nose down")
	phase of surface elevation at moment of cylinder impact
ω	angular velocity of lifeboat ($= \phi'$)
$',''$	first and second time derivative.

1. INTRODUCTION

FREE-FALL lifeboats provide a safe alternative to conventional lifeboats for emergency evacuation from ships and offshore platforms. Although the concept is rather old, as evinced by a patent issued in 1897 and the first known application in 1961, there are few technical papers on the topic. Larsen (1979) gave a general overview of the concept. Nelson *et al.* published a few articles (1988, 1989a,b) on the kinematics of the boat during the fall and the effects of impact on the occupants. No references were found in the literature to any analytical or numerical method for predicting the motion of the boat during water entry.

In 1989 the Nederlandse Aardolie Maatschappij (NAM), an Operating Company within the Shell Group, started a programme of replacement and improvement of the means of emergency evacuation on nine offshore platforms. On these platforms 11 free-fall lifeboats will be installed during 1990–1991. The drop height of these boats, following from the necessary deck clearances, is to be just under 20 m and the platforms are in an area with adverse weather conditions.

With this project under way and possible future plans for installing similar boats on platforms with even larger deck clearances and in harsher environments, there is a need for a practical method of predicting the launch behaviour of these boats and to assess the risk of injury to the occupants. In particular, methods for evaluating the effects of waves and changes in the design of the boat and launch installation are desirable. In the first article on this launch simulation method (Boef, 1992), the theory of the hydrodynamic impact has been reviewed and the equations of motion for the water entry of a lifeboat were derived. This paper discusses the implementation of the total launch simulation, evaluation criteria and some applications.

2. LAUNCH SIMULATION OF FREE-FALL LIFEBOAT

There are two commonly used methods for launching free-fall lifeboats: boats mounted on a sloped launch cradle slide off the cradle after release, and boats hanging from a hook drop vertically after release. The cradle system is applied by, for example, Verhoef Aluminium Scheepsbouwindustrie B.V., while others have adopted the vertical drop. Figure 1 gives a schematic view of these systems.

The launch from a cradle can be divided into four different stages: (1)—the boat sliding along the launch skid, (2)—the rotation of the boat at the end of the skid, (3)—the free fall and (4)—the penetration into the water. In this section the equations of motion are derived for all four stages and reformulated for a numerical integration scheme. For practical reasons the launch simulation model is two-dimensional only: the motion is assumed to be purely in the plane of symmetry of the boat.

The intended installations on the NAM platforms all have cradle launching, and so emphasis was put on this launch mechanism. The resulting formulation, however, also covers the release from a hook: stages (1) and (2) can then simply be omitted.

2.1. *Sliding along the cradle*

Different systems can be devised for the sliding mechanism, but they all utilise a set of rollers on the cradle over which the boat rolls down. The line of contact has been defined with respect to the centre of gravity of the boat (cog) and the contact forces are assumed to act at both ends of this line (see Fig. 2). When the boat is released it will start sliding along the skid and the equations of motion are:

$$M \cdot x'' = F_{wx} + (F_{n1}+F_{n2}) \cdot (\cos\phi - S_{fr} \cdot \sin\phi) \tag{1}$$

$$M \cdot z'' = F_{wz} - M \cdot g + (F_{n1}+F_{n2}) \cdot (\sin\phi + S_{fr} \cdot \cos\phi) \tag{2}$$

$$I \cdot \phi'' = M_w + F_{n1} \cdot (B_{xx}+S_{fr} \cdot B_z) + F_{n2} \cdot (-B_{x2}+S_{fr} \cdot B_z) \tag{3}$$

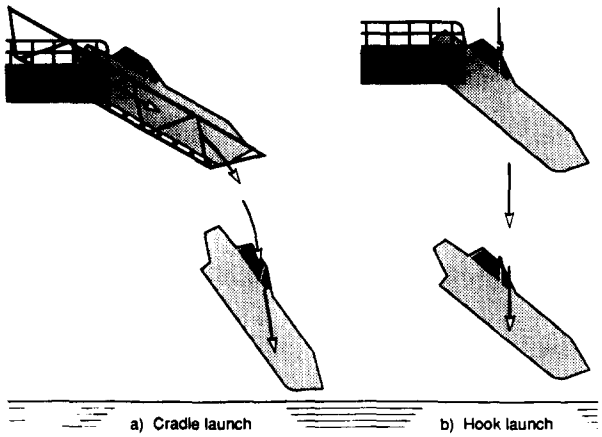

FIG. 1. Different launch options for free-fall lifeboat.

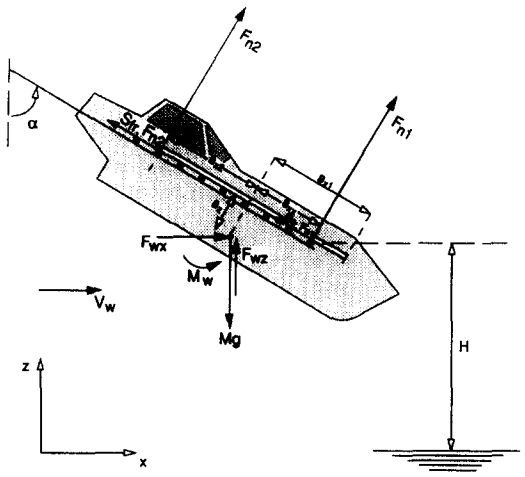

FIG. 2. Boat sliding along launch cradle.

where M and I are the mass and moment of inertia of the boat and F_{wx}, F_{wz} and M_w are the components of the drag in air. B_{xx} is the (varying) distance along the boat axis between the cog and the contact point near the bow:

$$B_{xx} = \min(B_{x1}, SL - [z(t=0) - z(t)]/\cos\alpha]) \; . \tag{4}$$

There are two kinematic constraints to ensure sliding:

$$\phi = \alpha \tag{5}$$

$$x' = z' \cdot \tan\alpha \; . \tag{6}$$

From Equations (1)–(6) the contact forces between the boat and skid can be solved:

$$F_{n1} = [F_n \cdot (B_{x2} - B_z \cdot S_{fr}) - M_w]/(B_{xx} + B_{x2}) \tag{7}$$

$$F_{n2} = [F_n \cdot (B_{xx} + B_z \cdot S_{fr}) + M_w]/(B_{xx} + B_{x2}) \tag{8}$$

where:

$$F_n = F_{n1} + F_{n2} = (M \cdot \boldsymbol{g} - F_{wz}) \cdot \sin\alpha - F_{wx} \cdot \cos\alpha \; . \tag{9}$$

The boat slides along the skid without rotation as long as $F_{n2} \geq 0$. In the solution procedure it is more convenient to have a criterion based on the displacement of the boat. This can be derived by substituting Equations (4), (8) and (9) in the condition above:

$$z(t=0) - z(t) < (SL + B_z \cdot S_{fr} + M_w/F_n) \cdot \cos\alpha \; . \tag{10}$$

By the elimination of the contact forces, the equations of motion can be written in a form suitable for numerical integration:

$$x' = v_x \tag{11a}$$

$$z' = v_z \tag{11b}$$

$$\phi' = \omega \tag{11c}$$

$$v_x' = [F_{wx} + F_n \cdot (\cos\alpha - S_{fr} \cdot \sin\alpha)]/M \tag{11d}$$

$$v_z' = [F_{wz} - M \cdot \boldsymbol{g} + F_n \cdot (\sin\alpha + S_{fr} \cdot \cos\alpha)]/M \tag{11e}$$

$$\omega' = 0 \, . \tag{11f}$$

Equations (11a)–(11c) are the three additional differential equations to reduce the equations of motion to a system of first-order differential equations. They are identical for all subsequent stages and will therefore not be repeated.

For the integration of this resulting system of first-order differential equations, a Runge–Kutta scheme with automatic step-size control, as described by Press *et al.* (1987), has been used. This method proved to be very suitable for solving the equations of motions during the impact at water entry and was therefore adopted for the entire launch simulation.

In this sliding stage the boat gains kinetic energy by acceleration along the boat axis. The velocity at the end of this stage strongly affects the subsequent behaviour. If it is too low, the boat will tumble over the end of the cradle and can end upside down.

2.2. *Rotation at skid end*

When condition (10) is no longer fulfilled, the boat starts rotating around the end of the skid (see Fig. 3). This will continue until there is no contact left between boat and cradle. In pratice contact will be lost as soon as $B_{xx} < -B_{x2}$, or, in terms of displacements, when:

$$z(t{=}0) - z(t) < SL \cdot \cos\alpha + B_z \cdot (\sin\phi - \sin\alpha) + B_{x2} \cdot \cos\phi \, . \tag{12}$$

The equations of motion are:

$$M \cdot x'' = F_{wx} + F_{n1} \cdot (\cos\phi - S_{fr} \cdot \sin\phi) \tag{13}$$

$$M \cdot z'' = F_{wz} - M \cdot \boldsymbol{g} + F_{n1} \cdot (\sin\phi + S_{fr} \cdot \cos\phi) \tag{14}$$

$$I \cdot \phi'' = M_w + F_{n1} \cdot (B_{xx} + S_{fr} \cdot B_z) \, . \tag{15}$$

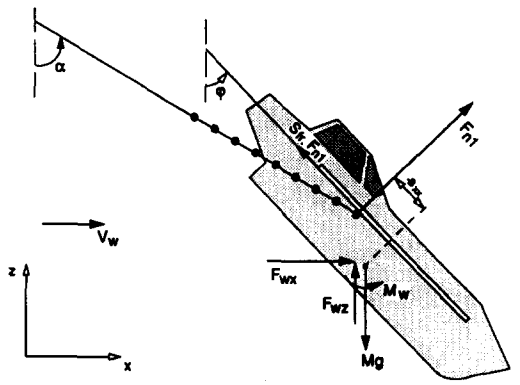

FIG. 3. Boat rotating at the end of the launch cradle.

During the rotation there is one kinematic constraint, forcing the boat to stay in contact with the end of the skid: the velocity of the boat at the point of contact is along the axis of the boat:

$$0 = z' \cdot \sin\phi + x' \cdot \cos\phi + \phi' \cdot B_{xx} \,. \tag{16}$$

B_{xx} can be expressed as a function of the vertical displacement of the cog:

$$B_{xx} = [z(t) - z(0) + SL \cdot \cos\alpha + B_z \cdot (\sin\phi - \sin\alpha)]/\cos\phi \,. \tag{17}$$

With the substitution of Equations (16) and (17) and their first derivatives into (13)–(15) the contact force F_{n1} can be explicitly expressed as a function of the external forces and the motion of the boat:

$$F_{n1} = [\phi' \cdot (x' \cdot \sin\phi - z' \cdot \cos\phi - B'_{xx}) - (F_{wx} \cdot \cos\phi + (F_{wz} - M \cdot \boldsymbol{g}) \cdot \sin\phi) / M - M_w/I]/[B_{xx} \cdot (B_{xx} + B_z \cdot S_{fr})/I + 1/M] \,. \tag{18}$$

With Equations (17) and (18) the equations of motion can be rewritten in a suitable form for solving numerically:

$$v'_x = [F_{wx} + F_{n1} \cdot (\cos\phi - S_{fr} \cdot \sin\phi)]/M \tag{19a}$$

$$v'_z = [F_{wz} - M \cdot \boldsymbol{g} + F_{n1} \cdot (\sin\phi + S_{fr} \cdot \cos\phi)]/M \tag{19b}$$

$$\omega' = [M_w + F_{n1} \cdot (B_{xx} + B_z \cdot S_{fr})]/I \,. \tag{19c}$$

In this second stage the horizontal and vertical momenta increase further and the boat starts to rotate. This rotation is important since it determines the angle of attack at the water surface.

2.3. *Free fall*

The equations of motions during free fall are very simple. The only forces acting on the boat are gravity and the wind force (drag):

$$v'_x = F_{wx}/M \tag{20a}$$

$$v'_z = F_{wz}/M - \boldsymbol{g} \tag{20b}$$

$$\omega' = M_w/I \,. \tag{20c}$$

The forces and moment due to air drag have been accounted for by the following approximation:

$$F_{wx} = -F_{wax} \cdot \sin\phi - F_{wnor} \cdot \cos\phi \tag{21}$$

$$F_{wz} = F_{wax} \cdot \cos\phi - F_{wnor} \cdot \sin\phi \tag{22}$$

$$M_w = F_{wax} \cdot L_{wax} - F_{wnor} \cdot L_{wnor} \tag{23}$$

with:

$$F_{wax} = C_{da} \cdot A_{da} \cdot \rho_w \cdot (v_{ax} - v_w \cdot \sin\phi) \cdot |v_{ax} - v_w \cdot \sin\phi|/2 \tag{24}$$

$$F_{wnor} = C_{dn} \cdot A_{dn} \cdot \rho_w \cdot (v_{nor} - v_w \cos\phi) \cdot |v_{nor} - v_w \cos\phi| / 2 \tag{25}$$

$$v_{ax} = x' \cdot \sin\phi - z' \cdot \cos\phi \tag{26}$$

$$v_{nor} = x' \cdot \cos\phi + z' \cdot \sin\phi \ . \tag{27}$$

In these equations ρ_w is the density of air and v_w is the wind velocity (positive in $+x$-direction). C_{da}, A_{da}, C_{dn} and A_{dn} are the drag coefficient and projected area of the boat for the axial direction and the direction normal to the axis, respectively. L_{wax} and L_{wnor} are the distances between the cog and the line of action of the axial and normal drag force, respectively. The effect of the rotation of the boat on the air drag has been ignored.

Except for conditions with large drop heights and/or high wind speeds, the influence of the air drag is insignificant. Ignoring this influence results in only an increase of vertical momentum due to the gravity force. The horizontal and angular velocities of the boat remain constant. The rotation of the boat during the free fall is very important as it determines the angle of attack at water entry.

2.4. *Penetration of water surface*

From the first instant of contact with the water surface onwards the equations of motion are dominated by the force between the boat and the surrounding water and the gravity force. The force exerted on the boat by the water during entry can be split into the following contributions (see Fig. 4):

- a vertical force proportional to the immersed volume of the boat, the buoyancy and wave inertia, F_{buoy};
- a force normal to the boat axis due to the momentum transfer, F_{mom};
- a force along the boat axis due to momentum transfer and to drag, F_{axm} and F_{drag}.

These forces due to momentum transfer contain terms that are proportional to the accelerations of the boat. The inertia terms appear separately in the equations as added mass components. This results in a completely filled asymmetrical mass matrix. Thus the fluid inertia terms couple the three motions (vertical, horizontal and rotational).

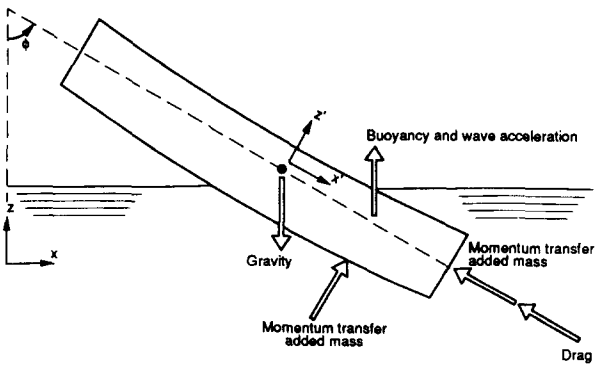

FIG. 4. Forces on lifeboat at water entry.

The derivation of the fluid forces is discussed extensively in Part I of this paper (Boef, 1992). The equations of motion become:

$$\begin{vmatrix} v_x' \\ v_z' \\ \omega' \end{vmatrix} = \begin{vmatrix} M+m_{11} & m_{12} & m_{13} \\ m_{21} & M+m_{22} & m_{23} \\ m_{31} & m_{32} & I+m_{33} \end{vmatrix}^{-1} \cdot \begin{vmatrix} Fx_{mom}+F_{axm}+Fx_{\text{drag}} \\ -M\cdot g+F_{axm}+F_{\text{buoy}}+Fz_{mom}+Fz_{\text{drag}} \\ FM_{\text{buoy}}+FM_{mom} \end{vmatrix} \cdot \quad (28a, 28b, 28c)$$

For all the forces not in the direction of the boat axis the contribution for each cross-section is calculated and numerically integrated over the length of the boat. For this integration Simpson's scheme with a variable number of intervals was implemented and proved to be perfectly adequate. The coupled system of equations also requires the inversion of the mass matrix at every time step. For this purpose an LU decomposition and backsubstitution routine for asymmetrical matrices was added. All numerical calculations were based on routines given by Press *et al.* (1987).

3. RESPONSE OF A HUMAN BODY TO IMPACT

Of major concern in the application of free-fall lifeboats are the potentially high accelerations of the boat at water entry and the associated risk of injury to the occupants. A straightforward way to judge the effects of the impact is to compare the actual acceleration field at the occupants' seats with defined acceleration limits. These limits then correspond to a certain risk of injury. In establishing a procedure of this kind one faces several problems:

- acceleration limits (magnitude) in themselves have virtually no meaning. It is the combination of magnitude and duration that affects the human body;
- for many injuries (e.g. spinal) the type of support of the body affects the allowable limit. A body in a well-designed boat seat can withstand considerably higher accelerations than in a ordinary car.
- the occupant of the boat is not subjected to an acceleration in one direction only, but to a combined acceleration field;
- proper experimental data are limited.

Nelson *et al.* (1989b) give a clear review of the various methods for evaluating the effects of the accelerations on the occupants of the lifeboat. On the basis of their exposée it was decided not to use an evaluation criterion with acceleration limits, but to adopt the dynamic response model as presented by Brinkley (1984).

This model has been used by the U.S. Air Force for evaluating the effects of accelerations on pilots during ejection from an aircraft. The model assumes that human response in each coordinate direction of the acceleration field at the seat (see Fig. 5), can be characterised as an independent, single degree-of-freedom mass-spring system subjected to base accelerations (see Fig. 6). Appropriate mass, spring and dashpot properties have been established by research at the Air Force Aerospace Medical Research Laboratory. These values, based on a representative male in a fully restrained seat, are presented in Table 1.

As discussed by Nelson *et al.* (1989b), the risk of injury level resulting from an acceleration in one of the coordinate directions is directly related to one response

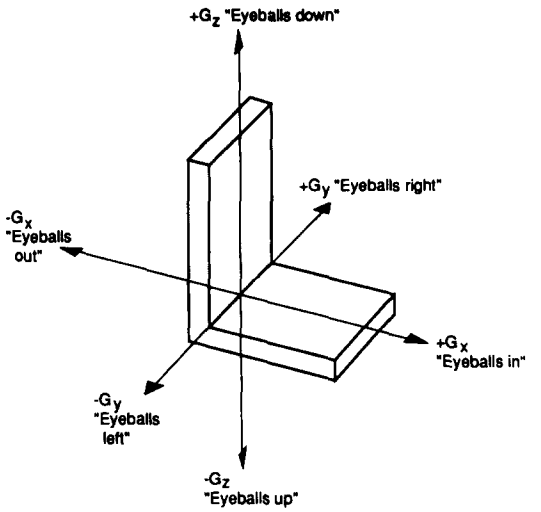

FIG. 5. Coordinate systems for accelerations on the human body.

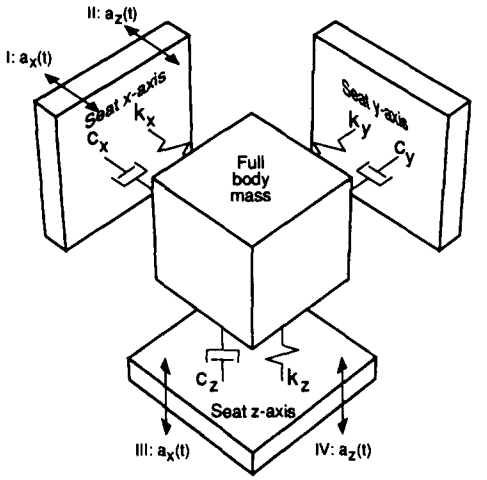

FIG. 6. Definition of the four basic body response calculations.

TABLE 1. MODEL PARAMETERS OF BODY-SEAT MODEL

Direction	Natural frequency (rad/sec)	Body mass (kg)	Stiffness (N/m)	Damping (kg/sec)	Damping ratio
X (eyeballs in/out)	62.8	75	0.30×10^6	942	0.100
Y (eyeballs left/right)	58.0	75	0.25×10^6	783	0.090
Z (eyeballs up/down)	52.9	75	0.21×10^6	1777	0.224

parameter of the model, the maximum displacement between body and seat. Nelson *et al.* propose two sets of allowable displacements, corresponding to different risk levels, the lower one for training and the higher one for emergency evacuations. They are listed in Table 2.

Though the absolute values of the limits might be disputable, the method provides an excellent basis for the comparison of different launches. It combines the magnitude and duration of the acceleration peaks into one parameter, the displacement, and is supported by experiments for fully restrained seats, comparable with the type used in any well-designed free-fall lifeboat. The method can also easily be extended to evaluate the effects of multi-axis accelerations by using the combined dynamic response ratio (CDRR). The CDRR is computed by:

$$\mathrm{CDRR}(t) = [(\delta_x(t)/S_x)^2 + (\delta_y(t)/S_y)^2 + (\delta_z(t)/S_z)^2]^{1/2} \tag{29}$$

where $\delta(t)$ is the actual (calculated) relative displacement and S the allowable one as defined in Table 2. The choice of S (training or emergency) defines the application for which we wish to evaluate the combined field. The associated risk level is not exceeded as long as CDRR ≤ 1.0.

The implementation of the dynamic response model can be divided into three steps: firstly, calculation of the acceleration field at the set foundation for a number of seat positions; secondly, the calculation of the relative displacements between body and seat in all three directions; finally, combining these displacements in the CDRR.

During the launch analysis of the lifeboat, the motions, velocities and accelerations of the centre of gravity of the boat are recorded. These data are used in a postprocessor for dynamic response analysis to derive the accelerations at the seat foundations for different locations. If it is assumed that the boat behaves as a rigid body, this is a simple derivation:

$$a_x = v'_x \cdot \sin\phi - v'_z \cdot \cos\phi - (s_s - s_{cog}) \cdot \omega^2 \tag{30a}$$

TABLE 2. ACCEPTANCE CRITERIA OF DYNAMIC RESPONSE MODEL (ALLOWABLE DISPLACEMENTS BETWEEN BODY AND SEAT)

	Displacement (cm)	
Direction*	Training	Emergency
$+X$ (eyeballs out)	7.0	8.7
$-X$ (eyeballs in)	7.0	8.7
$+Y$ (eyeballs left)	4.1	5.0
$-Y$ (eyeballs right)	4.1	5.0
$+Z$ (eyeballs up)	3.2	4.2
$-Z$ (eyeballs down)	5.3	6.3

*Note that the signs of the displacements are opposite to the signs of the accelerations: an acceleration in the $+X$ direction (eyeballs in) causes a displacement in the $-X$ direction.

$$a_z = -v_x' \cdot \cos\phi - v_z' \cdot \sin\phi - (s_s - s_{cog}) \cdot \omega' \tag{30b}$$

where s_s defines the position of the seat with respect to the stern.

These accelerations are defined in the (moving) boat's coordinate system. Although it is theoretically more sound to use the seat motion relative to the global (fixed) coordinate system, this approach results in accelerations that can directly be compared with accelerometer data from measurements. In addition, measured accelerations can be used in the response calculations without adjustments to the coding.

The procedure for calculating the relative displacements in this study differs slightly from the approach of Nelson *et al.* (1989b). To avoid repetition of the calculations for different options of seat orientation, the displacements in body x- and z-directions (y-direction is disregarded in two-dimensional analysis) are calculated for two seat orientations, $\phi = 0^0$ and $\phi = 90^0$ (see Fig. 7). This results in four relative displacements:

$$\phi = 0^0 : \delta_{xx}(t) = \delta_x(t; a_x) \tag{31a}$$

$$\delta_{zz}(t) = \delta_z(t; a_z) \tag{31b}$$

$$\phi = 90^0 : \delta_{xz}(t) = \delta_x(t; a_z) \tag{31c}$$

$$\delta_{zx}(t) = \delta_z(t; a_x) \, . \tag{31d}$$

Rather than using the iterative solution procedure of Nelson *et al.* (1989b), we adopted a direct integration with Runge–Kutta's method for calculating (31). The system of equations for δ_{xx}, for example, becomes:

$$d(\delta_{xx})/dt = v_{xx} \tag{32a}$$

$$d(v_{xx})/dt = -a_x(t) - (c_x \cdot v_{xx} + k_x \cdot \delta_{xx})/m \, . \tag{32b}$$

In these equations m is the body mass and c_x and k_x are the damping and stiffness in the x-direction as defined in Table 1.

The actual displacements for the various seat orientations (see Fig. 7), can now be obtained simply by linear superposition. For a forward-facing seat at an angle ϕ with the vertical we obtain:

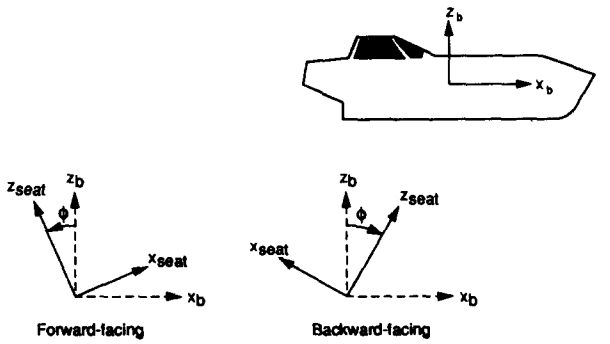

FIG. 7. Definition of seat orientation and seat-coordinate system.

$$\delta_{x\phi} = \delta_{xx} \cdot \cos\phi + \delta_{xz}\sin\phi \tag{33a}$$

$$\delta_{z\phi} = -\delta_{zx} \cdot \sin\phi + \delta_{zz}\cos\phi \tag{33b}$$

and for a backward-facing seat at an angle ϕ:

$$\delta_{x\phi} = -\delta_{xx} \cdot \cos\phi + \delta_{xz}\sin\phi \tag{34a}$$

$$\delta_{z}\phi = \delta_{zx} \cdot \sin\phi + \delta_{zz}\cos\phi \; . \tag{34b}$$

For every seat orientation the displacements can now be combined in the CDRR:

$$\mathrm{CDRR}_{\phi}(t) = [(\delta_{x\phi}(t)/S_x)^2 + (\delta_{y\phi}(t)/S_y)^2 + (\delta_{z\phi}(t)/S_z)^2]^{1/2} \; . \tag{35}$$

Although $\delta_{y\phi}$ is not included in the two-dimensional analysis, an estimated (constant) value, derived, for example, from measurements, can be included to account for effects in the y-direction. If the CDRR of a certain seat position and orientation is smaller than 1.0 during the launch and impact time span, then the level of risk of injury, associated with the S-values, is not exceeded.

4. COMPARISON BETWEEN SIMULATION AND FULL-SCALE MODEL TEST

In July 1988 a series of full-scale tests were conducted with an FL50 lifeboat, manufactured by Verhoef Aluminium B.V., in the Rotterdam harbour. Figures 8 and 9 show the measured accelerations and the corresponding (training) CDRRs for the stern and bow seats, respectively. These acceleration components and CDRRs are for seats in an upright position, facing backwards. The drop height was 27 m and the test was repeated twice, resulting in a spread of the acceleration of approximately 10%. Tests with drop heights of 31 and 35 m showed a similar response, but with higher peaks, as can be expected.

These test data were very valuable in validating our model. An example of the input data for the numerical simulations is listed in Table 3. Although there was no time available to check the sensitivity of the results to variations of all the parameters used, the deadrise angle and the curvature of the keel line turned out to be important parameters with major effects on the trajectory of the boat after impact and on the corresponding decelerations. These parameters were estimated as accurately as possible from the lines-plan of the FL50.

Figure 10 shows the calculated trajectory of the axis of the boat during fall and impact. The boat disappears just below the surface, as observed during the tests, and leaves the water again with the bow upward and some forward velocity. Detailed experimental data are not currently available to enable the predicted exit to be confirmed.

In Fig. 11 the x- and z-acceleration (in the coordinate system of the boat) are displayed for the stern, mid- and bow seats (the mid-seat corresponding to the cog). The predictions agree quite well with the measurements, although there are also clear differences. The peaks at first impact are a little higher, while the response after this first peak is milder than that observed in the measurements. Several effects may cause these differences: the inertia moment of the boat was not known precisely, the geometry of the boat is simplified in the model, particularly in the bow section, the bow of the model is less streamlined than the bow of the real boat. The last factor might explain

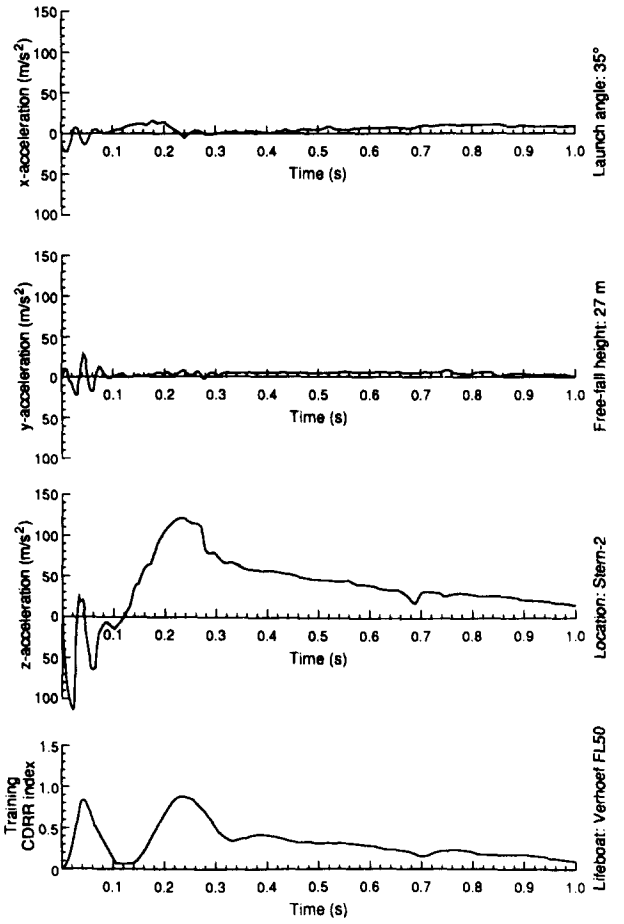

FIG. 8. Measured accelerations and CDRR for stern seat FL50.

the "larger" impact at first entrance. Further, effects such as the flexibility of the boat hull and air-cushioning are not included.

The same conclusions are applicable to the calculated CDRRs (see Fig. 12). The values are similar, but the test results show slightly larger CDRRs at the bow, while the numerical analysis resulted in larger CDRRs at the stern. This difference most probably arises from the simplified boat geometry in the model; this leads to a different distribution of added mass and therefore different forces and a shift of the instantaneous points of rotation. An additional source for the differences in this case is the different numerical integration used to obtain the CDRRs. The time integration of the measured acceleration, according to the model of Nelson *et al.* (1989b), probably introduces some numerical damping and might affect the peak values to some extent.

Figure 12 also shows the CDRRs for forward-facing seats, inclined at an angle of 75° to the vertical. The graphs clearly indicate the advantages of this seat positioning over seats in the upright position. Exactly the same conclusion was arrived at from the re-

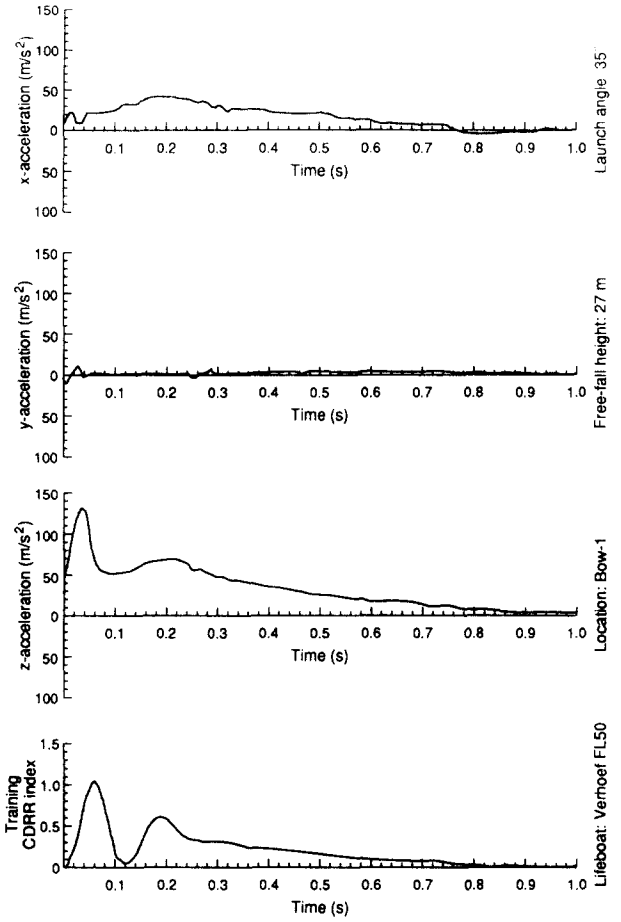

FIG. 9. Measured accelerations and CDRR for bow seat FL50.

TABLE 3. DATA OF NUMERICAL MODEL FL50 LIFEBOAT

Mass of boat and occupants	M	10,200 kg
Moment of inertia boat and occupants	I	41,000 kg.m² (estimated)
Length of boat model	L	9.4 m
Deadrise angle	β	30°
Height of wedge cross-section	$BH1$	0.87 m
Height of rectangular cross-section	$BH2$	0.98 m
Width of boat model		3.20 m
Volume of boat model		40 m³
Distance from cog to stern	BS_{cog}	4.20 m
Distance from cog to keel	BH_{cog}	1.20 m
Curvature of keel line	B_{cur}	0.60 m
Height of slide bar above the cog	B_z	−1.20 m
Start of slide bar (to cog)	B_{x1}	4.00 m
End of slide bar (to cog)	B_{x2}	4.60 m
Skid angle with vertical	α	55°
Skid height	H	27 m
Distance skid end to cog of boat	SL	5.1 m
Friction factor between skid and boat	Sfr	0.05

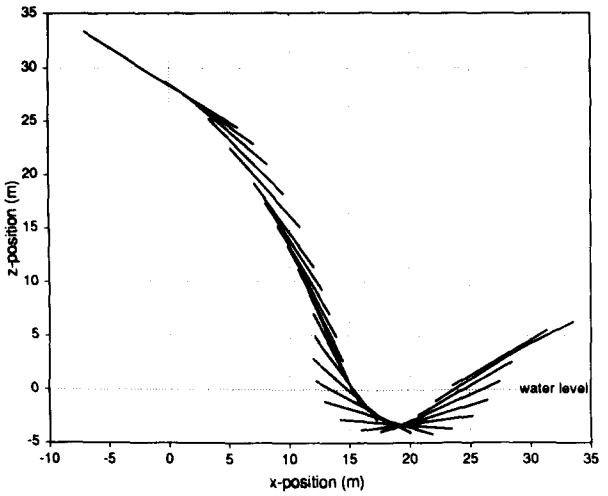

FIG. 10. Trajectory of FL50 dropped from 27 m.

analysis of the CDRRs for this seat orientation from the full-scale measurements.

The important conclusion of this comparison between simulation and full-scale measurements is that, although the mathematical model is not perfect, the agreement is sufficiently good to meet our objective: a simple and quick means for predicting the effect of waves and design changes on the impact and its effect on the occupants. It is very likely that by modelling the boat geometry in more detail an even better agreement will be obtained.

5. CASE STUDY

Most of the lifeboats that will be installed by NAM are of the FL30 type. Therefore this boat was selected for the evaluation of the launch under a number of wave conditions. The launch into still water was analysed first; the input data for this analysis are summarised in Table 4. This analysis was followed by three launches into a wave of 8 m amplitude and a period of 13 sec. This wave is the most probable maximum wave for the different platform locations with a chance of occurrence of once in 5 yr. Figure 13 gives an overview of the conditions analysed.

Figures 14–16 show the trajectory of the boat axis during the launch into still water, the accelerations at the seat foundations (stern, cog, bow) and the training CDRRs for the stern and bow seats, respectively; the CDRR at the cog is only a fraction of those at the ends of the boat and will not be discussed. The CDRRs for the seats in the upright position (facing backwards) are acceptable, but a considerable reduction can be achieved by placing the seats at a 75° angle (facing forwards). This design change was proposed by the manufacturer. For the stern seat, the most critical location, a 50% reduction will be achieved. Table 5 summarises the most important response parameters for the various launches.

When the three launches into the wave at different phase angles are compared (see Table 5), the following observations can be made: for launches into both the trough ($\phi = -\pi/2$) and the rising water surface ($\phi = -\pi/4$, $\phi = 0$) the acceleration peaks

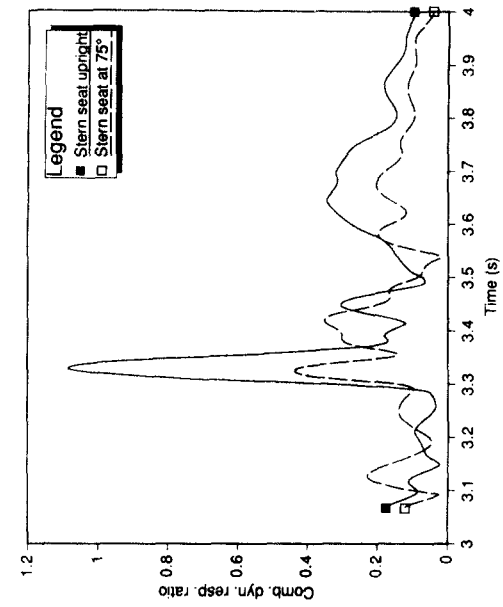

FIG. 12. CDRRs for seat positions at stern and bow.

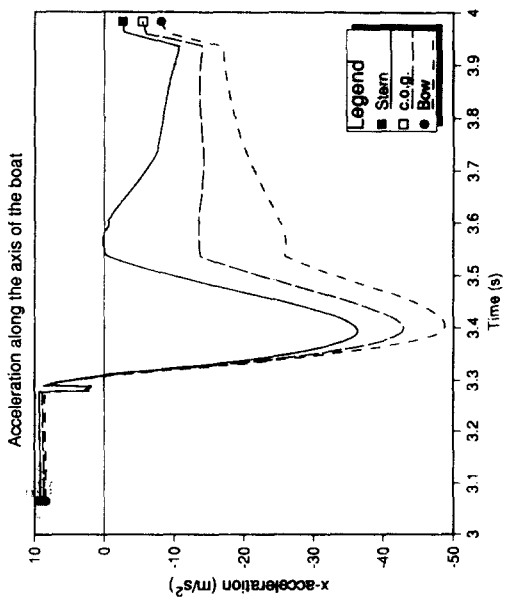

FIG. 11. Accelerations for FL50 dropped from 27 m.

TABLE 4. DATA OF NUMERICAL MODEL FL30 LIFEBOAT

Mass of boat and occupants	M	6870 kg
Moment of inertia boat and occupants	I	20,000 kg.m^2 (estimated)
Length of boat model	L	8.5 m
Dead-rise angle	β	30°
Height of wedge cross-section	$BH1$	0.81 m
Height of rectangular cross-section	$BH2$	0.86 m
Width of boat model		2.80 m
Volume of boat model		30 m^3
Distance from cog to stern	BS_{cog}	3.75 m
Distance from cog to keel	BH_{cog}	1.10 m
Curvature of keel line	B_{cur}	0.50 m
Height of slide bar above the cog	B_z	0.35 m
Start of slide bar (to cog)	B_{x1}	1.95 m
End of slide bar (to cog)	B_{x2}	3.20 m
Skid angle with vertical	α	55°
Skid height	H	19 m
Distance skid end to cog of boat	SL	5.8 m
Friction factor between skid and boat	Sfr	0.05

increase considerably, by more than 50%, when compared to still water. The CDRRs, however, increase to a lesser extent. This can be explained by the fact that the body displacements are a function of the combined acceleration field (peaks do not occur simultaneously) and any change of duration of the acceleration peaks. The worst impact conditions clearly occur when the rising surface is hit, and not in the trough. The

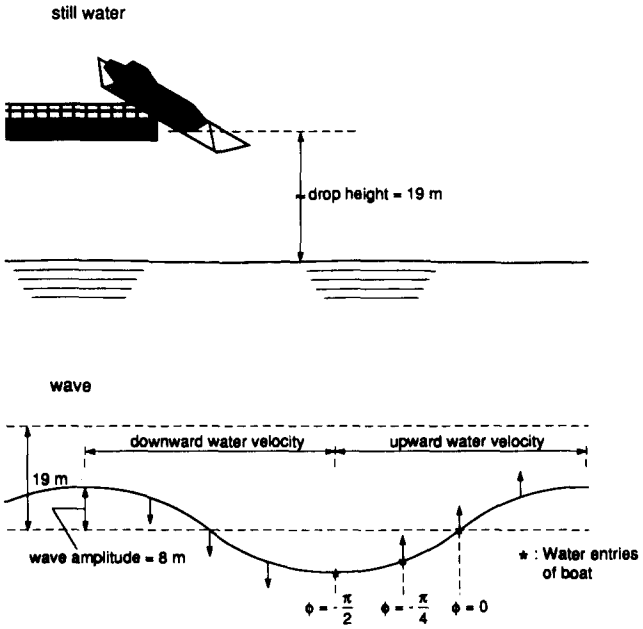

FIG. 13. Definition of height and water entries of FL30 launch simulations.

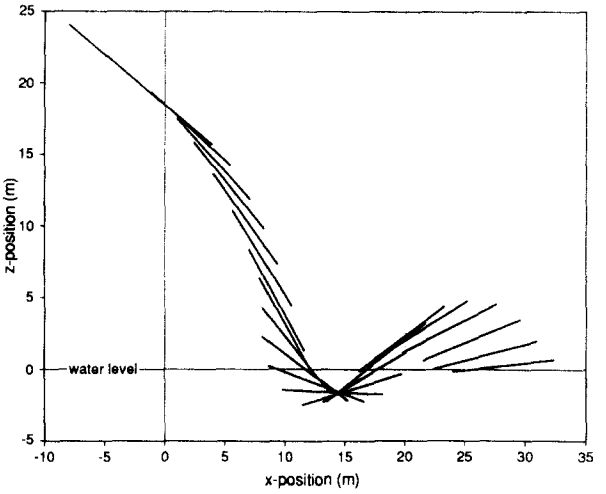

Fig. 14. Trajectory of FL30 dropped from 19 m.

upward water velocity and the larger angle of the boat with the vertical (angle of attack) exceed the effect of the additional drop height in the trough entry.

It must be emphasised that only the vertical motion of the water has been included in the model. This simplification will definitely affect the prediction of the path of the boat after water entry, but is probably less relevant for the modelling of the impact itself. The impact force of an object is proportional to the relative velocity (between

Table 5. Results of FL30 launch analysis

Conditions	Still water	Wave*		
Wave phase (ϕ)	–	$-\pi/2$	$-\pi/4$	0
Total drop height (m)	19.0	27.0	24.7	19.0
Upward water velocity (m/sec)	0.0	0.0	2.7	3.9
Boat angle at entrance (°)	32.2	25.3	27.2	32.2
Vertical velocity (m/sec)	17.1	21.0	20.0	17.1
Horizontal velocity (m/sec)	7.2	7.2	7.2	7.2
Maximum acceleration (m/sec)				
Axial bow	42	60	67	60
Axial stern	24	41	42	29
Normal bow	140	190	245	230
Normal stern	95	130	160	150
Angular (rad/sec^2)	51	70	87	80
CDRR training				
Bow seat 0°	0.81	0.92	1.12	1.20
Bow seat 75°	0.58	0.64	0.81	0.84
Stern seat 0°	0.95	1.02	1.22	1.32
Stern seat 75°	0.47	0.51	0.61	0.65

*Wave amplitude 8.0 m, period 13 sec.

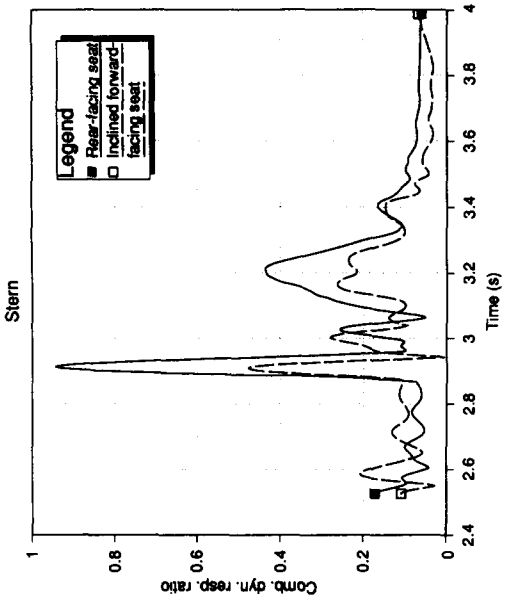

FIG. 16. CDRRs for upright seats and rotated seats at bow and stern of FL30.

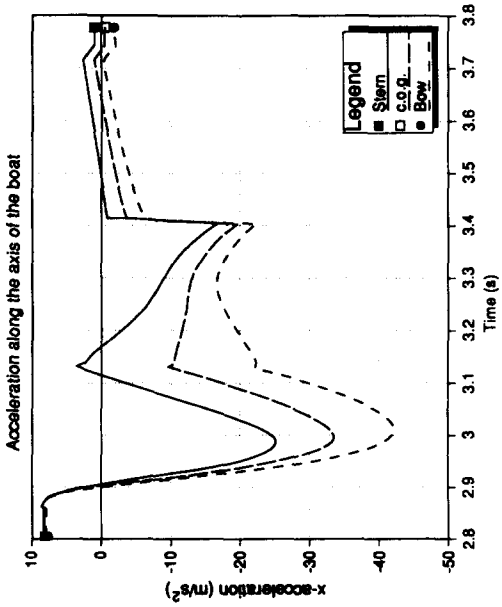

FIG. 15. Accelerations for FL30 dropped from 19 m.

object and water) squared. The boat has the highest velocity in the vertical direction and therefore the effect of the horizontal water velocity will be smaller than that of the vertical water velocity. The same applies to the effect of the wave slope; wave slopes are normally too small to affect the impact.

From the assessment of the resulting CDRRs, the advantage of the 75° orientation of the seats is obvious. The maximum response ratio is 66% of the maximum ratio in the upright position. This effect is particularly important for the bow and stern seats, the worst positions; for the seats around the centre of the boat there is hardly any difference between the two orientations. If space requirements prohibit a 75° orientation for all seats, a more efficient combination of seat orientations might be considered.

It should be noted that all the CDRRs reflect the acceptable risk level for training. The acceptable risk levels for emergency allow about another 25% on the displacements (see Table 2). This would mean that the emergency CDRRs for the upright seats will be around 1.0, which is near the acceptance limit, but for the inclined seats it is much lower.

In summary it can be concluded for this case study that the boat meets the risk requirements for emergency evacuation with either seat orientation even in the most adverse weather conditions in the application area. The inclined orientation is definitely preferable. Regular training in bad weather should be discouraged.

It should be noted however, that in the assessment of the acceptability and applicability of the free-fall concept these risk evaluations do not stand on their own. To obtain a fair appraisal of the free-fall concept for a specific application the risk should be compared with the risks associated with other means of emergency evacuation.

6. CONCLUSIONS

A theoretical model has been derived for all stages of the launch of a free-fall lifeboat. It is applicable both to launches from a cradle and from a hook. With some simplifications of the boat geometry and the selection of efficient numerical schemes, this resulted in an efficient tool for the simulation of these launches, requiring limited input data.

Comparison of the numerical results with full-scale measurements of launch tests with an FL50 lifeboat shows reasonably good agreement and gives confidence in the numerical approach.

For an FL30 boat launched from a height of 19 m, comparison was made between the entry into still water and into waves. Launching the boat into a wave of 8 m amplitude will increase the acceleration levels in the boat by up to 50%, but these levels do not exceed the acceptance criteria. The worst entry conditions occur when the water surface is rising from the wave trough to the mean sea level.

Changing the seat orientation in the FL30 for upright and facing backwards to a 75° angle with the vertical and facing forwards will decrease the risk of injury to the occupants. For the bow and stern seats the combined dynamic response ratios (CDRRs) reduce by 30 and 50%, respectively.

The numerical model provides a means of evaluating and improving free-fall lifeboat arrangements. In particular, for installations on platforms with larger deck clearances and a harsher environment, for which the boat impact will be more critical, significant benefits can be obtained from such an analysis.

Though the numerical model gave acceptable results, it is still rather simplified. Additional work is desirable to improve the computational model (a more detailed description of the geometry of the boat and of the water kinematics) and also to validate its predictions against (model) experiments. A full three-dimensional model of the boat and the environment might be the ultimate goal, but would require considerable effort.

Acknowledgements—The author wishes to thank the Nederlandse Aardolie Maatschappij and Shell International Research Maatschappij for their support of this work. He is also indebted to Verhoef Aluminium Scheepsbouwindustrie B.V. for their kind permission to make use of their boat data and test results.

REFERENCES

BOEF, W.J.C. 1992. Launch and impact of free-fall lifeboats. Part I: Impact theory. *Ocean Engng* **19**, 119–138.

BRINKLEY, J.W. 1984. Personnel protection concepts for advanced escape system design. *AGARD Conference Proceedings, Human Factors Consideration in High Performance Aircraft.*

LARSEN, P. 1979. A new dimension in life saving at sea—a systematic approach to a new abandonment system. Norwegian Maritime Research, Report No. 1.

NELSON, J.K., HIRSCH, T.J. and MAGILL, J.M. 1988. Measured accelerations on free-fall lifeboats. *Trans. ASME* **110**.

NELSON, J.K., HIRSCH, T.J. and PHILLIPS, N.S. 1989b. Evaluation of occupants accelerations in lifeboats. *Trans. ASME* **111.**

NELSON, J.K., HIRSCH, T.J. and WANG, J. 1989a. Determining kinematics of free-fall lifeboats from measured accelerations. *Proceedings of the 8th International Conference on Offshore Mechanics and Arctic Engineering, The Hague, March 1989.*

PRESS, W.H., FLANNERY, B.P., TEUKOLSKY, S.A. and VETTERLING, W.T. 1987. *Numerical Recipes: the Art of Scientific Computing.* Cambridge University Press, Cambridge.